Niveoporofomes (Basidiomycota, Fomitopsidaceae) in Tropical Africa: Niveoporofomes oboensis sp. nov. and N.widdringtoniae comb. nov., two species from Afromontane Forests

Cony Antonio Decock
Universite Catholique de Louvain
Leif Ryvarden
University of Oslo: Universitetet i Oslo
Mario Amalfi (mario.amalfi@botanicgardenmeise.be)
Meise Botanic Garden https://orcid.org/0000-0002-1792-7828

Research Article

Keywords: Afromontane ranges, Basidiomycota, Fomitopsis, polypores, phylogeny, taxonomy

Posted Date: September 30th, 2021

DOI: https://doi.org/10.21203/rs.3.rs-927746/v1

Abstract

During a survey of polypores in the montane forest of the Ôbo de São Tomé National Park, in the western African, equatorial island of São Tomé, a specimen that was, *a priori*, related to *Fomitopsis*, based on the gross morphology of the basidiome and a brown rot, showed deviating features including subglobose basidiospores with a large gutta, what pointed toward *Niveoporofomes*. Phylogenetic inferences based on multiple loci dataset (ITS-nLSU-nSSU-*tef1-rpb2*) confirmed these affinities, and *Niveoporofomes oboensis* is described as new. The species is compared to *Fomitopsis widdringtoniae*, known from southeast Africa, which is characterized also by subglobose basidiospores; hence, the new combination *N. widdringtoniae* is proposed. The new combination *Niveoporofomes globosporus* (basionym *Trametes globospora*) is also proposed based on phylogenetic analyses. A key to the species of *Fomitopsis*, *Niveoporofomes*, *Rhodofomes*, and *Rhodofomitopsis* in Tropical Africa is presented.

Introduction

Fomitopsidaceae, typified by *Fomitopsis* P. Karst., is a family of brown rot polypores, mostly spanning over temperate areas (Han et al. 2016; Justo et al. 2017). The family (also referred to as the *Antrodia* clade) was revised by Han et al. (2016) and *Fomitopsis*, as accepted by then (or *sensu lato*, e.g., Ryvarden and Johansen 1980), was shown to be polyphyletic. Consequently, *Fomitopsis* species were reclassified into several new or reinstated genera, including *Fragifomes, Niveoporofomes, Rhodofomes, Rhodofomitopsis*, or still *Rubellofomes* (Han et al. 2016).

In tropical Africa, *Fomitopsis* s.l. were represented by seven species (Ryvarden and Johansen 1980; Masuka and Ryvarden 1993; Mossebo and Ryvarden 1997). However, considering the current treatment of *Fomitopsidaceae* (Han et al. 2016), *Rhodofomes* and *Rhodofomitopsis* occur also in Tropical Africa, represented by *Rhodofomes carneus* (as *Fomitopsis carnea* (Blume & T. Nees) Imazeki, Ryvarden and Johansen 1980) and *Rhodofomitopsis africana* (as *Fomitopsis africana* Mossebo & Ryvarden, Mossebo and Ryvarden 1997).

As part of an ongoing survey of polypores (Basidiomycota) in sub-Saharan Africa (Decock and Mossebo 2001, 2002; Decock 2001, 2007, 2011a, b; Decock and Ryvarden 2002, 2015, 2020; Decock and Masuka 2003; Decock et al. 2005, 2021; Amalfi et al. 2010; Yombiyeni et al. 2011; Decock and Bitew 2012), a specimen from the African, equatorial island of São Tomé, collected at Ôbo de São Tomé National Park, was shown to belong to *Niveoporofomes* based on morphology and [ITS-nLSU-nSSU-*tef1-α-rpb2*]-based phylogenetic inferences. It is interpreted as representing a distinct, undescribed species, proposed as *Niveoporofomes oboensis*. This species is compared to *Fomitopsis widdringtoniae* Masuka & Ryvarden, known from south-eastern Africa, which has identical basidiospores (Masuka and Ryvarden 1993). A key to the species of *Fomitopsis*, *Niveoporofomes*, *Rhodofomes*, and *Rhodofomitopsis* in Tropical Africa is presented.

Niveoporofomes has been proposed to host *Fomitopsis spraguei*, a species that deviates from *Fomitopsis pinicola* and species of other related genera in having obovoid to broadly ellipsoid basidiospores with a large gutta. The genus was up to now considered monospecific (Han et al. 2016). Analyses of available ITS sequences showed that sensu Han et al. (2016), *N. spraguei* is not monophyletic, but encompasses several clades that could represent each a distinct species, of which *N. globosporus* that is proposed as a new combination.

Materials And Methods

Material and collection localities

The type specimen originated from mid-elevation forest at elev. ~1300 masl at Ôbo de São Tomé National Park in São Tomé, which vegetation is the Afromontane Equatorial rainforest (Carvalho et al. 2004). The type specimen is preserved at O, with isotypes at BR and MUCL (herbarium acronyms according to Thiers (Thiers 2016) continuously updated (http://sciweb.nybg.org/science2/IndexHerbariorum.asp).

Description

Colours are described according to Kornerup and Wanscher (Kornerup and Wanscher 1981). Sections were carefully dissected under a stereomicroscope in hot (40° C) NaOH 3% solution and later examined in NaOH 3% solution at room temperature (Decock et al. 2010). Sections were also examined in Melzer's reagent and lactic acid Cotton blue to show staining reaction. All the microscopic measurements were done in Melzer's reagent. In presenting the size range of several microscopic elements, 5% of the measurements at each end of the range are given in parentheses when relevant. In the text, the following abbreviations are used: av. = arithmetic mean, R = the ratio of length/width of basidiospores, and av_R = arithmetic mean of the ratio R.

Molecular study and phylogenetic analysis

DNA extraction, amplification and sequencing of the 5' end of the nuclear ribosomal 28S rRNA gene (region including the domains D1–D3), the ITS regions (including 5.8S), the nuclear SSU regions, partial tef1-alpha gene and the region between domains 6 and 7 of the second largest subunit of the RNA polymerase II (rpb2), were as described in Amalfi et al. (2012) and Han et al. (2016). The sequences were assembled in Geneious Pro v. 6.0.6 (Biomatters). Materials and sequences used in this study are listed in Table 1.

Table 1
List of species, collections, and sequences used in the phylogenetic analyses

Species name	Sample no.	Locality	GenBank accession numbers					References
			ITS	nLSU	nSSU	tef1	rpb2	
Antrodia juniperina	CBS 117.40	USA	DQ491416	AY515346	–	–	DQ491389	Kim et al. 2007
A.juniperina	0310 1a	USA	MG787606	MG787653	MG787782	MG787873	MG787831	Chen,Y.Y., Cui,B.K. and Dai,Y.C., Direct Submission
A. malicola	Harkonen K622	China	KU866261	–	–	KU866216	–	Spirin et al. 2016
A. malicola	X1016	China	KC595896	KC595896	–	–	–	Ortiz-Santana et al. 2013
A. malicola	Cui 9491	China	KT968824	KT968828	–	–	KT988994	Han et al. 2016
A. serialis Holotype	KHL 12010 (O)	Norway	JQ700292	JQ700292	–	–	–	Spirin et al. 2017
A. serialis Neopype	KHL 12010 (GB)	Norway	NR154676	JX109844	–	JX109898	JX109870	Binder et al 2013
Antrodia serialis	Otto Miettinen X732	Finland	JQ700271	JQ700271	–	–	–	Spirin et al. 2017
A. serialis	CBS 306.82	DQ491417	–	–	–	DQ491390	Kim et al. 2007	
A. serialis	Cui 10519	China	KP715307	KP715323	KR605911	KP715337	KR610830	Han et al. 2016
A. variiformis	CBS 309.82	USA	DQ491418	AY515344	–	–	DQ491391	Kim et al. 2007
A. variiformis	JV 0809/96	USA	KT995131	KT995154	MG787766	KU052736	MG787821	Spirin et al. 2017
Buglossoporus quercinus	LY BR 2030	France	KR605799	KR605738	KR605897	KR610728	KR610818	Han et al. 2016
B. americanus	JV1707_9J	Costa Rica	MN318452	–	–	–	–	Vlasák et al. 2016
B.eucalypticola	Dai 13660	China	KR605808	KR605747	KR605906	KR610736	KR610825	Han et al. 2016
B.pulvinus	CBS 858.72	Germany	DQ491419	MH872316	DQ491446	-	DQ491392	Kim et al. 2007
Daedalea africana	O 15372	Kenya	KP171196	KP171216	KR605871	KR610704	KR610795	Han et al. 2015, 2016
D. allantoidea	Dai 13612A	China	KR605795	KR605734	KR605892	KR610723	KR610813	Han et al. 2016
D. americana	JV 0312/24.7-J	USA	KP171197	KP171217	KR605872	KR610705	KR610796	Han et al. 2015, 2016
D. dochmia	CBS 426.84	Thailand	DQ491401	AY515326	–	–	DQ491374	Kim et al. 2007
D. modesta	Cui 10151	China	KP171205	KP171227	KR605883	KR610716	KR610806	Han et al. 2015, 2016
D. radiata	Cui 8575	China	KP171210	KP171233	KR605888	KR610720	KR610811	Han et al. 2015, 2016
Fomitopsis cana	Cui 6239	China	JX435777	JX435775	KR605826	KR610661	KR610761	Li et al. 2013, Han et al. 2016

Species name	Sample no.	Locality	GenBank accession numbers					References
			ITS	nLSU	nSSU	tef1	rpb2	
F. cana	Dai 9611	China	JX435776	JX435774	KR605825	KR610660	KR610762	Li et al. 2013, Han et al. 2016
F. durescens	Overholts 4215	USA	KF937293	KF937295	KR605835	–	–	Han et al. 2014, 2016
F. durescens	Ryvarden 910796	Venezuela	KF937292	KF937294	KR605834	KR610669	KR610766	Han et al. 2014, 2016
F. hemitephra	O 10808	Australia	KR605770	KR605709	KR605841	KR610675	–	Han et al. 2016
F. meliae	Roberts GA863	United Kingdom	KR605775	KR605714	KR605848	KR610682	–	Han et al. 2016
F. meliae	Ryvarden 16893	Unknown	KR605776	KR605715	KR605849	KR610681	KR610775	Han et al. 2016
F. mounceae	CFMR:32TT	USA	KF169621	–	–	KF178346	KF169690	Haight et al. 2018
F. mounceae	CFMR:DR-301	USA	KF169625	–	–	KF178350	KF169694	Haight et al. 2018
F. mounceae	DAOM:73999	Canada	MH086784	MH086803				
F. nivosa	JV 0509/52-X	China	KR605779	KR605718	KR605853	KR610686	KR610777	Han et al. 2016
F. ochracea	CFMR:DLL-3	USA	KF169588	–	–	KF178313	KF169657	Haight et al. 2018
F. ochracea	DAOM:F3249B	Canada	MH086778	MH086797	–	–	–	Haight et al. 2018
F. ostreiformis	BCC23382	Thailand	FJ372684	FJ372706	–	–	–	Rungjindamai et al. 2008
F. palustris	Cui 7615	China	KR605780	KR605719	KR605855	KR610688	KR610779	Han et al. 2016
F. pinicola	AFTOL ID 770	Unknown	AY854083	AY684164	AY705967	AY885152	AY786056	Matheny and Hibbett, Assembling the Fungal Tree of Life, direct submission
F. pinicola	CFMR:LT:323	Estonia	KF169651	–	–	KF178376	KF169720	Haight et al. 2018
F. pinicola	Cui 10312	China	KR605781	KR605720	KR605856	KR610689	KR610780	Han et al. 2016
F. pinicola	CBS 169.31	Germany	MH855169	MH866615	–	–	–	Vu et al. 2019
F. schrenkii	FP-105881-R	USA	KF169641	–	–	KF178366	KF169710	Haight et al. 2018
F. schrenkii	CFMR:JEH-142-ss12	USA	KF169642	–	–	KF178367	KF169711	Haight et al. 2018
F. subtropica	Cui 10181	China	JQ067653	JX435773	KR605866	KR610700	KR610790	Li et al. 2013, Han et al. 2016
F. subtropica	Cui 10578	China	KR605787	KR605726	KR605867	KR610698	KR610791	Han et al. 2016
Fragifomes niveomarginatus	Cui 10108	China	KR605778	KR605717	KR605851	KR610684	KR610776	Han et al. 2016
F. niveomarginatus	Wei 5583	China	HQ693994	KC507175	KR605852	KR610685	–	Han and Cui 2015, Han et al. 2016

Species name	Sample no.	Locality	GenBank accession numbers					References
			ITS	nLSU	nSSU	tef1	rpb2	
Neolentiporus maculatissimus	Rajchenberg 158	Unknown	–	AF518632	AF334921	–	AY218497	Hibbett and Binder 2002, Wang et al. 2004
Niveoporofomes globosporus **comb nov Holotype**	**M.C. Aime 3413**	**Belize**	**KC017760**	**KC017762**	**–**	**–**	**–**	Ryvarden et al. (2009)
Niveoporofomes globosporus **comb nov**	**S-20**	**Mexico**	**KR135353**	**–**	**–**	**–**	**–**	**Alfonso-Corrado,C. et al. unpublished**
Niveoporofomes oboensis **sp nov**	**MUCL 53518**	**Sao Tome**	**This study**	**This study**	**This study**	**This study**	**This study**	**This study**
Niveoporofomes spraguei	4638	France	KR605784	KR605723	KR605862	KR610696	KR610786	Han et al. 2016
N. spraguei	Cui 8969	China	KR605785	KR605724	KR605863	KR610695	KR610787	Han et al. 2016
N. spraguei	JV 0509/62	USA	KR605786	KR605725	KR605864	KR610697	KR610788	Han et al. 2016
N. spraguei	CBS 365.34	USA	DQ491406	MH867073	–	–	DQ491379	Kim et al. 2007
N. spraguei	C5	Unknown	JX434660	–	–	–	–	Chai,D.-D. direct submission
N. spraguei	Cui 8951	China	KC507164	KC507174	–	–	–	Han and Cui 2015
N. spraguei	X1430	China	KC595924	–	–	–	–	Ortiz-Santana et al. 2013
N. spraguei	KA12-1397	South Korea	KR673596	–	–	–	–	Kim et al. 2015
N. spraguei	SAT1224005	USA	KY777368	–	–	–	–	Matheny et al direct submission
N. spraguei	SAT1028304	USA	MG663257	–	–	–	–	Matheny et al direct submission
N. spraguei	CLZhao 2241	China	MH114658	–	–	–	–	Zhao,C.-L. direct submission
N. spraguei	S.D. Russell MycoMap 6609	USA	MK560112	–	–	–	–	Russell S.D. direct submission
N. spraguei	Mushroom Observer # 247114	USA	MK571181	–	–	–	–	Russell S.D. direct submission
N. spraguei	S.D. Russell MycoMap # 73	USA	MK575221	–	–	–	–	Russell S.D. direct submission
N. spraguei	S.D. Russell MycoMap # 1318	USA	MK575222	–	–	–	–	Russell S.D. direct submission
N. spraguei	S.D. Russell MycoMap # 105	USA	MK575223	–	–	–	–	Russell S.D. direct submission
Pilatoporus ibericus	O 10810	Portugal	KR605771	KR605710	KR605842	KR610676	KR610771	Han et al. 2016
P. ibericus	O 10811	Italy	KR605772	KR605711	KR605843	KR610677	KR610772	Han et al. 2016
Piptoporus betulinus	CBS 377.51	Japan	MH856908	MH86843	–	–	–	Vu et al. 2019

Species name	Sample no.	Locality	GenBank accession numbers					References
			ITS	nLSU	nSSU	tef1	rpb2	
	CBS 378.51	Austria	DQ491423	DQ491423	–	–	–	Kim et al. 2007
P. betulinus	Dai 12665	China	KP171215	KP171238	KR605896	KR610724	KR610817	Han et al. 2015, 2016
P. betulinus	Miettinen 12388	Finland	JX109856	JX109856	–	JX109913	JX109884	Binder at al. 2013
Rhodofomes cajanderi	Cui 9879	China	KC507157	KC507167	KR605827	KR610663	KR610763	Han and Cui 2015, Han et al. 2016
R. cajanderi	Cui 9888	China	KC507156	KC507166	KR605828	KR610662	KR610764	Han and Cui 2015, Han et al. 2016
R. cajanderi	JV 0410/14a,b-J	USA	KR605768	KR605707	KR605829	KR610664	–	Han et al. 2016
R. cajanderi	CBS 142.25	USA	MH854818	–	–	–	–	Vu et al. 2019
R. carnea	Ryvarden 10118	Tanzania	KF999921	KF999925	KR605831	KR610666	–	Han and Cui 2015, Han et al. 2016
R. incarnatus	Cui 10348	China	KC844848	KC844853	KR605844	KR610679	KR610773	Han and Cui 2015, Han et al. 2016
R. rosea	JV 1110/9	Czech Republic	KR605783	KR605722	KR605861	KR610694	KR610785	Han et al. 2016
R. subfeei	Cui 9229	China	KR605789	KR605728	KR605869	KR610701	KR610793	Han et al. 2016
Rhodofomitopsis africana	MUCL 43284	Cameroon	DQ491422	–	–	–	DQ491395	Kim et al. 2007
Rh. africana	Isolate 6537	India	MG430342	–	–	–	–	Saroj,P et al. direct submission
Rh. cupreorosea	CBS 236.87	Costa Rica	DQ491400	AY515325	–	–	DQ491373	Kim et al. 2007
Rh. feei	JV 0610/K9-Kout	Mexico	KF999922	KF999926	KR605836 a	KR610673 a	–	Han and Cui 2015, Han et al. 2016
Rh. feei	Oinonen 6011906	Brazil	KC844851	KC844856	KR605837	KR610671	KR610767	Han and Cui 2015, Han et al. 2016
Rh. feei	Ryvarden 14115	Costa Rica	KF999923	KF999927	–	–	–	Han and Cui 2015
Rh. feei	Ryvarden 42928	Australia	KF999924	KF999928	KR605839	KR610672	KR610769	Han and Cui 2015, Han et al. 2016
Rh. feei	Ryvarden 37603	Venezuela	KC844850	KC844855	KR605838	KR610670	KR610768	Han and Cui 2015, Han et al. 2016
Rh. lilacinogilva	CBS 422.84	Australia	DQ491403	–	DQ491430	–	DQ491376	Kim et al. 2007
Rh. lilacinogilva	Schigel 5193	Australia	KR605773	KR605712	KR605846	KR610680	KR610774	Han et al. 2016
Rubellofomes cystidiatus	Cui 5481	China	KF937288	KF937291	KR605832	KR610667	KR610765	Han et al. 2014, 2016
Ru. cystidiatus	Yuan 6304	China	KR605769	KR605708	KR605833	KR610668	–	Han et al. 2016

Species name	Sample no.	Locality	GenBank accession numbers					References
			ITS	nLSU	nSSU	tef1	rpb2	
Ungulidaedalea fragilis	Cui 10919	China	KF937286	KF937290	KR605840	KR610674	KR610770	Han et al. 2014, 2016

Nucleotide sequences were automatically aligned using the MUSCLE algorithm (Edgar 2004) with default settings. The alignment was further optimised and manually adjusted as necessary by direct examination with the software Se-Al v. 2.0a11 (University of Oxford).

Two datasets were constructed and used for further phylogenetic analyses respectively at family and genus level. A combined dataset combined nuclear ribosomal partial LSU, ITS-5.8S, and SSU, partial *tef1-α*, and rpb2 genes sequences from 75 collections (Online Resource 1), including the outgroup (*Neolentiporus maculatissimus* strain Rajchenberg 158, (Han et al. 2016)). A second dataset combined the ITS-5.8S sequences of 23 collections (Online Resource 2), including all nineteen *Niveoporofomes* sequences available in public databases (based on a > 95.0% sequence similarity threshold, on 22/04/2021), with *Piptoporus betulinus* strain (CBS 378.51) as outgroup (Han et al. 2016).

The assignment of codon positions in the protein-coding sequences was confirmed by translating nucleotide sequences into predicted amino acid sequences using Mac-Clade 4.0 (Maddison and Maddison 2005) and then compared with the annotated *Fomitopsis pinicola* isolate AFTOL-ID 770 sequences.

Potential ambiguously aligned segments, especially in the introns present in tef-1 and in the ITS-5.8S alignment, were detected by Gblocks v0.91b (Castresana 2000) (http://molevol.cmima.csic.es/castresana/Gblocks.html), with the following parameter settings: minimum number of sequences for a conserved position = 38 (minimum possible); minimum number of sequences for a flank position = 38 (minimum possible); maximum number of contiguous non-conserved positions = 4 bp, minimum block size = 4 bp, and gaps allowed within selected blocks in half of the sequences.

To detect the possible bias from substitution saturation and to evaluate the phylogenetic signal, we tested each partition of the combined dataset and the ITS-5.8S dataset by using Xia's test (Xia et al. 2003; Xia and Lemey 2009), as implemented in DAMBE (Xia and Xie 2001). As the Iss.c is based on simulation results, there is a problem with more than 32 species. To circumvent this problem, DAMBE was used to randomly sample subsets of 4, 8, 16 and 32 OTUs multiple times and to perform the test for each subset to see if substitution saturation exists for these subsets of sequences. In order to confirm the results of the Xia's method, we also plotted the raw number of transversions and transitions against Tamura-Nei genetic distances with the aid of the DAMBE package, with an asymptotic relationship indicating the presence of saturation. Models of evolution for BI were estimated using the Akaike Information Criterion (AIC) as implemented in Modeltest 3.7 (Posada and Crandall 1998). The combined dataset was subdivided into 7 data partitions: ITS, nuc-LSU, Nuc-SSU, *tef1-α* 1st and 2nd codon positions, *tef1-α* 3rd codon positions, and rpb2 1st and 2nd codon positions, and rpb2 3rd codon positions. The three introns present in *tef1-α* and the one present at the end of *rpb2* sequences were excluded from the phylogenetic inferences because judged too ambiguous to be confidently aligned (*tef1-α*) or because were missing in most of the sequences (*rpb2*). Phylogenetic analyses were performed separately for each individual and concatenated loci using Bayesian Inference (BI) as implemented in MrBayes v3. 2 (Ronquist et al. 2011) and Maximum Likelihood (ML) as implemented in RAxML 7.2.7 (Stamatakis et al. 2008). The best-fit models for each partition were implemented as partition specific models within partitioned mixed-model analyses of the combined dataset (Table 2). All parameters were unlinked across partitions. Bayesian analyses were implemented with two independent runs, each with four simultaneous independent chains for six million generations for both combined and ITS datasets, starting from random trees and keeping one tree every 1000th generation. All trees sampled after convergence (average standard deviation of split frequencies < 0.01 and confirmed using Tracer v1.4 (Rambaut and Drummond 2007) were used to reconstruct a 50% majority-rule consensus tree (BC) and to calculate Bayesian Posterior Probabilities (BPP). BPP of each node was estimated based on the frequency at which the node was resolved amongst the sampled trees with the consensus option of 50% majority-rule (Simmons et al. 2004). A probability of 0.95 was considered significant. Maximum Likelihood (ML) searches conducted with RAxML involved 1000 replicates under the GTRGAMMAI model, with all model parameters estimated by the programme. In addition, 1000 bootstrap (ML BS) replicates were run with the same GTRGAMMAI model. We provided an additional alignment partition file to force RAxML software to search for a separate evolution model for each dataset. Clades with Maximum Likelihood bootstrap values of 75% or greater were considered supported by the data.

Table 2
Summary of data sets used for phylogenetic inferences.

Datasets										
Properties	*tef1* 1st & 2nd	*tef1* 3rd	*tef1* introns	*rpb2* 1st & 2nd	*rpb2* 3rd	*rpb2* intron	nucSSU	nucLSU	ITS	ITS-5.8S restricted
Alignment size	244	121	208	432	216	76	83	1348	771	668
Excluded characters	-	-	208	-	-	76	-	-	369	-
Model selected	F81 + I + G	GTR + G	HKY + I + G	SYM + I + G	GTR + G	K80	GTR + I + G	GTR + I + G	GTR + I + G	GTR + G
- Likelihood score	1160.8060	2428.8706	3254.8496	2032.5619	3033.6099	237.5902	2041.7124	4516.7588	7215.0537	1653.3608
Base frequencies										
FrEq. A =	0.2993	0.0343	0.2138	Equal	0.2478	Equal	0.2726	0.2697	0.2346	0.2329
FrEq. C =	0.2284	0.4948	0.2421	Equal	0.1956	Equal	0.1900	0.2032	0.1762	0.2027
FrEq. G =	0.2639	0.2981	0.2087	Equal	0.2541	Equal	0.2593	0.2780	0.2206	0.2317
FrEq. T =	0.2085	0.1728	0.3354	Equal	0.3025	Equal	0.2780	0.2491	0.3686	0.3326
Proportion of invariable sites	0.8401	-	0.0591	0.6471	-	-	0.9082	0.6094	0.2125	-
Gamma shape	0.6822	0.8036	2.2345	0.5604	2.7065	-	2.1111	0.5410	0.6111	0.2537
Test of substitution saturation										
Iss	0.066	0.377	**1.157**	0.130	0.565	0.4635	0.020	0.292	0.169	0.0668
Iss.cSym	0.683	0.756	0.689	0.695	0.687	1.015	0.749	0.768	0.691	0.7417
P (Sym)	< 0.0001	< 0.0001	< 0.0001	< 0.0001	< 0.0001	< 0.0001	< 0.0001	< 0.0001	< 0.0001	< 0.0001
Iss.cAsym	0.359	0.499	0.372	0.367	0.633	1.067	0.444	0.479	0. 362	0.4961
P (Asym)	< 0.0001	< 0.0062	< 0.0001	< 0.0001	< 0.0436	< 0.0001	< 0.0001	< 0.0001	< 0.0001	< 0. 0001

Note: Iss: index of substitution saturation. Iss.cSym: critical value for symmetrical tree topology. Iss.cAsym: critical value for extremely assymetrical tree topology. P: probability that Iss is significantly different from the critical value (Iss.cSym or Iss.cAsym). Iss < Iss.c = no saturation, Iss > Iss.c = substantial saturation (very poor for phylogenetics)

To detect topological conflicts amongst data partitions, the nodes between the majority-rule consensus trees obtained in the ML analysis from the individual datasets were compared with the software compat.py (available at www.lutzonilab.net/downloads). Paired trees were examined for conflicts only involving nodes with ML BS > 75% (Mason-Gamer and Kellogg 1996; Reeb et al. 2004; Lutzoni et al. 2004). A conflict was assumed to be significant if two different relationships for the same set of taxa (one being monophyletic and the other not) were observed in rival trees. Sequence data and statistical analysis for each individual dataset and combined analysis are provided in Table 2.

Results

Phylogenetic analysis

By comparing the tree topologies obtained for the individual datasets, no significant conflict involving significantly supported nodes was found using the 75% ML BP criterion; the datasets were therefore combined.

The test of substitution saturation (Table 2) showed that the observed index of substitution saturation (*Iss*) for the restricted ITS-5.8S dataset, the *tef-1* (1st and 2nd codon positions, and 3rd codon position), *rpb2* (each codon positions), nucLSU and nucSSU alignments of the combined dataset was significantly lower than the corresponding critical index substitution saturation (*Iss.c*), indicating that there was little saturation in our sequences ($P < 0.001$). On the other hand, the ITS-5.8S partition of the combined dataset, the *tef-1* introns and the *rpb2* intron showed sign of substitution saturation, indicating the unsuitability of these data for phylogenetic analysis. Nevertheless, reanalysing the ITS partition with DAMBE after that Gblocks retained 402 sites (51% of a total of 771 sites), the substitution saturation test revealed an Iss value that was significantly ($P < 0.001$) lower than the Iss.c (Table 2), indicating the suitability of this data for further phylogenetic analysis. We therefore included the ITS-5.8S partition in the combined dataset, excluding the poorly aligned positions identified by Gblocks as well as the *tef-1* and the *rpb2* introns partitions.

The *Niveoporofomes s.s* ITS-5.8S dataset and the *Fomitopsis* s.l. combined [ITS-nLSU-nSSU-*tef1-α-rpb2*] data set comprised 23 and 75 taxa respectively including the outgroups and, once excluded the introns, were of 668 and 4149 sites long including gaps, respectively. Sequence data, evolutionary models and statistical analysis for each dataset are provided in Table 2. For the combined dataset the two Bayesian runs (6.000.000 generations) converged to stable likelihood values after 1.615.000 generations; therefore 4.385 stationary trees from each analysis were used to compute a 50% majority rule consensus tree in PAUP* to calculate posterior probabilities. For the ITS-5.8S dataset, the two Bayesian runs (4.000.000 generation) converged after 460.000 generations, and 3.540 stationary trees from each analysis were used to compute a 50% majority rule consensus tree in PAUP* to calculate posterior probabilities.

In the ML searches, the ITS-5.8S alignment had 154 distinct patterns with a proportion of gaps and undetermined characters of 11.95%. In the ML searches with RAxML, the combined dataset alignment had 1530 distinct patterns with a proportion of gaps and undetermined characters of 37.99%. The consensus of the BI and the Maximum Likelihood tree were nearly identical. The BI consensus trees for the combined and ITS-5.8S only datasets are presented in Figs. 1 and 2 respectively. The topologies of the trees regarding the recovery and the relative positions of the different taxa of the *Fomitopsis* complex were, overall, similar in all the phylogenetic inferences, and in accordance with previous published results (Ortiz-Santana et al. 2013; Han et al. 2016), at least for what concerns significantly supported branches.

The phylogenetic analyses recovered our specimen from Ôbo de São Tomé National Park in the vicinity of *N. spraguei*, forming a distinct branch (Fig. 1). On this basis and morphological characters, of which the

subglobose, obovoid basidiospores with a large gutta, the specimen is interpreted as representing an undescribed species proposed below as *Niveoporofomes oboensis*.

The collections of *N. spraguei*, available on GenBank, segregated into three clades (Fig. 2). The collections originating from USA and a single one from Europe clustered in a sister position to a clade that includes sequences from the holotype of *Trametes globospora* Ryvarden & Aime (Belize, Ryvarden et al. 2009) and two other collections from Mexico (KR135353, JX434660). The *N. spraguei* collections originating from Asia formed a third basal clade, suggesting that they represent a likely cryptic species.

Taxonomy

Niveoporofomes oboensis Decock, Amalfi & Ryvarden nov. sp. (MB 841205) Fig. 3.

Niveoporofomes oboensis is characterized by the combination of a pileate, slightly decurrent basidiome, a white pore surface, discolouring to brownish on bruising when fresh, 3.5–4 pores / mm, a pseudodimitic to dimitic hyphal system with hyaline clamped generative hyphae, dominated in the contextual trama by sclerified, thick-walled, septate, and clamped hyphae, with long aseptate segment and dominated in the hymenophoral trama by skeletal hyphae, and broadly obovoid to subglobose basidiospores with a large gutta, mostly 4.7–5.5 × 4.0–4.5 (–4.8) µm (ave = 5.2 × 4.3 µm).

Holotype: São Tomé, Ôbo de São Tomé National Park, on the way to Lagoa Amelia, approx. N 00°16.95' – E 006°35.48', elev. 1300 masl, on buttress of a living tree, *Olea capensis* (Oleaceae), 12 April 2011, Cony Decock, ST-11-04, Holotype in O, Isotypes in BR and MUCL (MUCL53518) (living strain ex holotype MUCL 53518).

Basidiome annual, pileate, with a slightly decurrent pore surface, corky when fresh, drying hard corky to woody; *pileus* solitary or imbricated with to 2 pilei superposed, broadly attached, elongated, 16–20 cm wide, projecting 8–9.5 cm, applanate in section, 1.5–2 cm thick at the base down to 0.5 at the margin; *pileus surface* white toward the margin, cinnamon to light brown, dark brown to black toward the base, glabrous; *margin* round, whitish, discolouring to brownish on bruising, drying dark greyish; *pore surface* plane to slightly concave, or wavy, whitish when fresh, drying whitish to pale corky; *pores* mostly round, 180–238 (–250) µm diam (ave 208 µm) to elliptic, 225–285 × 150–200 µm (ave 251 × 186 µm, 3.5–4 / mm; *dissepiments* thick, entire, 35–135 µm (ave 66 µm); *context* white, ivory when fresh or dry, dense and hard corky, fibrous, up to 10 mm thick at the base down to 2 mm at the margin; *tube layer* contrasting with the context, yellow white to orange white, pale corky, up to 13 mm high.

Hyphal system pseudodimitic (intermediate sensu Pegler 1996) to dimitic; *generative hyphae* in all parts hyaline, thin- to slightly thick-walled, with clamped septa, little branched, 2.0–2.5 µm diam; *context* dominated by sclerified, thick-walled generative hyphae, (3.5–) 4.0–5.0 (–5.5) µm (ave 4.6 µm) in the main part, negative in Melzers reagent, acyanophilous, with large, basal and intermediate clamps, with "spouting" clamps, with aseptate segments of variable length, measured from 50 µm up to 350 µm, reverting to thin-walled generative hyphae or ending in an aborted thin-walled hyphae, or occasionally in a whip-like narrow, unbranched to little branched process; mediate hyphae uncertain; *hymenophoral trama* dominated by skeletal hyphae, originating from a basal clamp or a short mediate hyphae, from 2.2–2.5 µm at the basal septum to 3.0–4.0 (–4.5) µm (ave 3.6 µm) in the main part, measured up to 500 µm long, very thick-walled, hyaline, ending thin-walled, negative in Melzers reagent, acyanophilous, irregularly swelling in alkali.

Hymenium: *basidia* clavate to slightly pear-shaped, clamped at the basal septum, with four sterigmata; *basidioles* clavate to slightly pear-shaped, clamped at the basal septum, 16–20 × 6.5–8 µm; cystidioles very few, with a basal clamps, slightly ventricose, bottle-shaped, ~ 17 × 6.0 µm; *basidiospores* subglobose, broadly obovoid, hyaline, thin-walled, smooth, most with a large oil drop (best seen in fresh specimen), (4.5–) 4.7–5.5 (–5.7) × 4.0–4.5 (–4.8) µm (ave = 5.2 × 4.3 µm), R = 1.1–1.3 (ave R = 1.2).

Physiology (type of rot)

brown rot;

Ecology (substrate, host, habitat)

on buttress of a living tree, *Olea capensis* (Oleaceae), Afromontane Equatorial rainforest.

Distribution. Known from the type locality, Ôbo de São Tomé National Park, São Tomé.

Phylogenetic affinities

the sole known phylogenetic relative are, *hitherto*, *N. spraguei* and *T. globospora*.

Discussion

Niveoporofomes was segregated from *Fomitopsis* based on the subglobose to globose basidiospores, which are elliptic in *Fomitopsis* s.s. and related genera. Multilocus phylogenetic analyses confirmed that *N. spraguei* and *F. pinicola* were not monophyletic.

The hyphal system of *Niveoporofomes* was described as dimitic with "frequently branched" skeletal hyphae (Han et al. 2017). This description is of uncertain interpretation. To characterize skeletal hyphae as "frequently branched" is intrinsically contradictory; skeletal hyphae are, by definition, unbranched, but for the sparingly branched mediate hyphae (Corner 1932). Ryvarden and Melo (Ryvarden and Melo 2014) described the hyphal system as trimitic, with generative, skeletal, and binding hyphae. Rivoire (Rivoire 2020) provided a more accurate description of the hyphal system, dominated both in the context and the hymenophoral trama by thick-walled [sclerified] generative hyphae, with scarce "skeletal" and "binding" hyphae.

Niveoporofomes oboensis and *N. spraguei* share the hyphal system, as described by Rivoire (2020), the subglobose, obovoid basidiospores, and a brown rot. Multilocus phylogenetic inference also confirmed their closed affinities. *Niveoporofomes oboensis* differs from *N. spraguei* by a basidiome margin and pore surface tinting brownish when bruised in fresh conditions. These two species also have a disjoint autecology and distribution. The autecology of *N. oboensis*, including the host relationships, habitat, and distribution is known for the type specimen only; it was found on buttresses of *Olea capensis* at Ôbo de São Tomé National Park, in Afromontane Equatorial rainforest (White 1986; Carvalho et al. 2004), whereas *N. spraguei* grows mostly on *Quercus* and *Castanea* in Northern temperate areas (Gilbertson and Ryvarden 1993; Ryvarden and Gilbertson 1994; Ryvarden and Melo 2014; Rivoire 2020).

In tropical Africa, *F. widdringtoniae* (Masuka and Ryvarden 1993) is the closest morphological relative of *N. oboensis*. The species was described growing on *Widdringtonia nodiflora* (L.) Powrie, a South-eastern African, endemic Gymnosperm (Cupressaceae). It is known so far from Malawi only, but may follow its host southernly. It is characterized also by globose basidiospores (Masuka and Ryvarden 1993), what points toward *Niveoporofomes* rather than *Fomitopsis* s.s. Its phylogenetic affinities are unknown, but on the basis of the basidiospores shape and size, and a brown rot, we propose the new combination *Niveoporofomes widdringtoniae* (Masuka & Ryvarden) Decock & Ryvarden, comb. nov., MB839610 (basionym *F. widdringtoniae* Masuka & Ryvarden, Mycol. Helv. 5(2):145, 1993, MB359440).

Niveoporofomes oboensis differs from *N. widdringtoniae* in basidiome size (up to 20 cm wide vs up to 5 cm wide), 3.5–4 vs 7–8 pores / mm, slightly larger basidiospores 4.7–5.5 (–5.7) × 4.0–4.5 µm, averaging 5.2 × 4.3 µm vs 4.5-5 µm in diam, on average < 5 µm, and likely in host and distribution range.

Fomitopsis s.l. was represented in Tropical Africa by seven species, *F. africana*, *F. carneus*, *F. rhodophaea* (Lev.) Imazeki, *F. scutellata* (Schwein.) Bondartsev & Singer, *F. supina* (Sw.) Ryvarden, *F. widdringtoniae*, and *F. zuluensis* (Wakef.) Ryvarden (Ryvarden 1972; Ryvarden and Johansen 1980; Masuka and Ryvarden 1993; Mossebo and Ryvarden 1997). Currently, *F. zuluensis* would be the sole *Fomitopsis* s.s. recognized still in Tropical Africa, but its phylogenetic affinities are unknown for the time being. *Fomitopsis africana* and *F. carnea* are nowadays accepted in *Rhodofomitopsis* (*R. africana*) and *Rhodofomes* (*R. carneus*) (Han et al. 2016), whereas *F. widdringtoniae* is here accepted in *Niveoporofomes*, a genus now represented by two species in Tropical Africa.

Fomitopsis rhodophaea, *F. scutellata*, and *F. supina* belong to the white rot genera *Neofomitella* (Li et al. 2014b), *Datroniella* (Li et al. 2014a), and *Fomitella* (Li et al. 2014b), respectively. They are members of the core polyporoid clade (white rot species, Justo et al. 2017) and not of the *Antrodia* clade (brown rot species).

Brown rot polypores are little diversified in Tropical Africa. They are mostly found inhabiting highland forest ecosystems of Eastern Africa or the Albertine rift, and in the case of *N. oboensis*, a mountain area of western Insular Africa. The notable exception is *R. africana* that was originally described from lowland in Cameroon, on an African non-native host (*Eucalyptus*).

Key to the species of Fomitopsis, Niveoporofomes, Rhodofomitopsis, **and** Rhodofomes **found in sub-Saharan, continental and insular Africa.**

1. Context and pore surface distinctly pinkish (when fresh)……. 2

1' Context and pore surface white, ochraceous, beige, to golden brown…….. 3

2 Pores 3–4 per mm; pileus dark brown; basidiospores cylindrical to navicular …..*Rhodofomitopsis africana*

Known hitherto from the lowland rain forest of Cameroon.

2' Pores 5–7 per mm; pileus almost black; basidiospores cylindrical to allantoid……*Rhodofomes carneus*

Known from East Africa.

3 Pileus with a reddish to black cuticle; basidiospores elliptic 8–10 µm long……*Fomitopsis zuluensis*

Known *hitherto* from South Africa.

3’ Pileus without cuticle; basidiospores subglobose, obovoid, ≤ 6 µm diam in the longest dimension…….4

4 Pileus white, light to dark brown from the base, bruising greenish; known from *Olea capensis* (Oleaceae)

…… *Niveoporofomes oboensis*

Known *hitherto* from highlands of São Tomé.

4’ Pileus whitish with some greyish to dirty brown spots; known from *Widdringtonia* (Cupressaceae)……

……*Niveoporofomes widdringtoniae*

Known hitherto from the highlands of Malawi.

Notes on N. spraguei. *Niveoporofomes spraguei*, as currently accepted (Gilbertson and Ryvarden 1986; Ryvarden and Melo 2014; Han et al. 2016; Rivoire 2020), is a pan-temperate taxon in the Northern hemisphere, growing on various angiosperms, mostly *Quercus* and *Castanea*, both in Europe and North America (Gilbertson and Ryvarden 1986, Ryvarden and Melo 2014, Rivoire 2020).

The phylogenetic analyses based on ITS sequences available at GenBank separated specimens of *N. spraguei* into three clades; an East Asian (China and South Korea) clade, a North American / European clade, and a third, Mesoamerican clade, in an intermediate position, that comprises specimens originating from Mexico and Belize (Fig. 2). The North American / European clade should correspond to *N. spraguei* s.s., in which case, the East Asian clade could represent a distinct taxon. The Mesoamerican clade includes the type of *Trametes globospora*, a species that deviates from all other species of *Trametes* in having globose basidiospores, 4.5–6 µm diam (Ryvarden et al. 2009). Basidiospores are elliptic in all other species of *Trametes*. The new combination *Niveoporofomes globosporus* (Ryvarden & Aime) Decock, Amalfi & Ryvarden comb. nov. (MB839611) is proposed (basionym *Trametes globospora* Ryvarden & Aime, Synopsis Fungorum 26: 28, 2009, MB509818).

Declarations

Ethics approval and Consent to participate: Not applicable

Consent for publication: All authors are aware and agree with the submission of this manuscript.

Availability of data and materials: Scientific data concerning DNA sequences and DNA data sets are made as supplementary materials (Online Resource 1 and 2), the type specimen of *Niveoporofomes oboensis* sp. nov. is preserved at O, with isotypes at BR and MUCL (herbarium acronyms according to Thiers 2016)

Competing interests: The authors declare that they have no conflict of interest.

Funding information: Funding was provided to Cony Decock by Belgian State – Belgian Federal Science Policy (BELSPO), through the BCCM program; to Mario Amalfi by the Fédération Wallonie-Bruxelles and Botanic Garden Meise; funding was provided to Cony Decock by the FNRS through a FRFC project (FRFC # 2.4515.06).

Code availability: Not applicable

Authors' contributions: Mario Amalfi and Cony Decock contributed to the study conception and design. Material collections were performed by Cony Decock. Mario Amalfi produced the sequences and conducted the phylogenetic analyses. The first draft of the manuscript was written by Cony Decock and Mario Amalfi, and all authors commented on previous versions of the manuscript. All authors read and approved the final manuscript.

Acknowledgments: The authors warmly thank the Ministério de Plano e Desenvolvimento, Direcção de Agricultura e Pescas de São Tomé for granting permits to collect in the Obô de São Tomé National Park, and the staff of the Park, and Faustino Oliveira, director of the botanical garden at Bom Sucesso, for the help offered during the collecting trip in April 2011. Mr. Bastien Loloum, Zuntabawe Lda, is warmly thanks also for the logistic aspects of the collecting trip. Cony Decock gratefully acknowledges the financial support received from the Belgian State – Belgian Federal Science Policy and the Fonds de la Recherche Fondamentale Collective (FRFC # 2.4515.06 and FRFC # 2.4.544.10.F). Mario Amalfi gratefully acknowledges the financial support received from Meise Botanic Garden and the Fédération Wallonie-Bruxelles.

References

Amalfi M, Raymundo T, Valenzuela R, Decock C (2012) Fomitiporia cupressicola sp. nov., a parasite on Cupressus arizonica, and additional unnamed clades in the southern USA and northern Mexico, determined by multilocus phylogenetic analyses. Mycologia 104:880–893. https://doi.org/10.3852/11-

Amalfi M, Yombiyeni P, Decock C (2010) Fomitiporia in sub-Saharan Africa: morphology and multigene phylogenetic analysis support three new species from the Guineo-Congolian rainforest. Mycologia 102:1303–1317. https://doi.org/10.3852/09-083

Binder M, Justo A, Riley R, et al (2013) Phylogenetic and phylogenomic overview of the Polyporales. null 105:1350–1373. https://doi.org/10.3852/13-003

Carvalho S, de Oliveira F, Vaz H (2004) Situation des ressources génétiques forestières de la République démocratique de Sao-Tomé-et-Principe. Note thématique sur les ressources génétiques forestières.

Castresana J (2000) Selection of conserved blocks from multiple alignments for their use in phylogenetic analysis. Molecular Biology and Evolution 17:540

Corner EJH (1932) A Fomes with two systems of hyphae. Transactions of the British Mycological Society 17:51–81. https://doi.org/10.1016/S0007-1536(32)80026-4

Decock C (2001) Studies in Perenniporia (Basidiomycetes, Polypores): African Taxa I. Perenniporia dendrohyphidia and Perenniporia subdendrohyphidia. Systematics and Geography of Plants 71:45. https://doi.org/10.2307/3668752

Decock C (2007) On the genus Microporellus, with two new species and one recombination (M. papuensis spec. nov., M. adextrinoideus spec. nov., and M. terrestris comb. nov.)

Decock C (2011a) Studies in Perenniporia s. lat. (Basidiomycota). African taxa V: Perenniporia alboferruginea sp. nov. from Cameroon. Plant Ecology and Evolution 144:226–232. https://doi.org/10.5091/plecevo.2011.509

Decock C (2011b) Studies in Perenniporia s. l. (Polyporaceae): African Taxa VII. Truncospora oboensis sp. nov., an undescribed Species from High Elevation Cloud Forest of São Tome. Cryptogamie, Mycologie 32:383–390. https://doi.org/10.7872/crym.v32.iss4.2011.383

Decock C, Bitew A (2012) Studies in Perenniporia (Basidiomycota). African taxa VI. A new species and a new record of Perenniporia from the Ethiopian Afromontane forests. Plant Ecology and Evolution 145:272–278. https://doi.org/10.5091/plecevo.2012.628

Decock C, Bitew A, Castillo G (2005) Fomitiporia tenuis and Fomitiporia aethiopica (Basidiomycetes, Hymenochaetales), two undescribed species from the Ethiopian highlands: taxonomy and phylogeny. Mycologia 97:121–129. https://doi.org/10.1080/15572536.2006.11832845

Decock C, Masuka A (2003) Studies in Perenniporia (Basidiomycetes, Aphyllophorales): African Taxa IV. Perenniporia mundula and Its Presumed Taxonomic Synonym, Vanderbylia ungulata. Systematics and Geography of Plants 73:161–170. https://doi.org/10.2307/3668626

Decock C, Mossebo DC (2001) Studies in Perenniporia (Basidiomycetes, Aphyllophorales): African Taxa II. Perenniporia centrali-africana, a New Species from Cameroon. Systematics and Geography of Plants 71:607–612. https://doi.org/10.2307/3668705

Decock C, Mossebo DC (2002) Studies in Perenniporia (Basidiomycetes, Polyporaceae): African Taxa III. The New Species Perenniporia djaensis and Some Records of Perenniporia for the Dja Biosphere Reserve, Cameroon. Systematics and Geography of Plants 72:55–62

Decock C, Ryvarden L (2002) Two undescibed Microporellus species and notes on M. clemensiae , M. setigerus and M. subincarnatus . Czech Mycology 54:19–30. https://doi.org/10.33585/cmy.54104

Decock C, Ryvarden L (2015) Studies in Perenniporia s.l. African taxa 9: Perenniporia vanhullii sp. nov. from open woodlands. Synopsis Fungorum 33:43–49

Decock C, Ryvarden L (2020) Sinopsis fungorum 42. In: Aphyllophorales of Africa 41, Some polypores from Gabon., FUNGIFLORA. pp 5–15

Decock C, Valenzuela R, Castillo G (2010) Studies in Perenniporia s.l. Perenniporiella tepeitensis comb. nov., an Addition to Perenniporiella: evidence from morphological and molecular data. Cryptogamie Mycologie 31:419–429

Decock C, Wagara I, Alphonse BZ, Yombiyeni P (2021) Haploporus (Basidiomycota, Polyporales) in sub-Saharan Africa: Poria eichelbaumii, a long-forgotten name, is reinstated in Haploporus and H. grandisporus sp. nov. is proposed. Mycological Progress 20:. https://doi.org/10.1007/s11557-020-01660-x

Edgar RC (2004) MUSCLE: multiple sequence alignment with high accuracy and high throughput. Nucleic acids research 32:1792–1797. https://doi.org/10.1093/nar/gkh340

Gilbertson RL, Ryvarden L (1993) European polypores, part 1. Synopsis Fungorum 6:1–387

Gilbertson RL, Ryvarden L (1986) North American Polypores. 1. Abortiporus - Lindtneria. Fungiflora

Haight J-E, Nakasone K, Laursen G, et al (2019) Fomitopsis mounceae and F. schrenkii-two new species from North America in the F. pinicola complex. Mycologia 111:1–19. https://doi.org/10.1080/00275514.2018.1564449

Han M-L, Chen Y, Shen L, et al (2016) Taxonomy and phylogeny of the brown-rot fungi: Fomitopsis and its related genera. Fungal Diversity 80:. https://doi.org/10.1007/s13225-016-0364-y

Han M-L, Cui B-K (2015) Morphological characters and molecular data reveal a new species of Fomitopsis (Polyporales) from southern China. Mycoscience 56:168–176. https://doi.org/10.1016/j.myc.2014.05.004

Han M-L, Song J, Cui B-K (2014) Morphology and molecular phylogeny for two new species of Fomitopsis (Basidiomycota) from South China. Mycological Progress 13:905–914. https://doi.org/10.1007/s11557-014-0976-0

Han M-L, Vlasak J, Cui B-K (2015) Daedalea americana sp. nov. (Polyporales, Basidiomycota) evidenced by morphological characters and phylogenetic analysis. Phytotaxa 204:277–286. https://doi.org/10.11646/phytotaxa.204.4.4

Hibbett DS, Binder M (2002) Evolution of Complex Fruiting-Body Morphologies in Homobasidiomycetes. Proceedings: Biological Sciences 269:1963–1969

Justo A, Miettinen O, Floudas D, et al (2017) A revised family-level classification of the Polyporales (Basidiomycota). Fungal Biology 121:798–824. https://doi.org/10.1016/j.funbio.2017.05.010

Kim C, Jo J, Kwag Y-N, et al (2015) Mushroom Flora of Ulleung-gun and a Newly Recorded Bovista Species in the Republic of Korea. Mycobiology 43:239. https://doi.org/10.5941/MYCO.2015.43.3.239

Kim KM, Lee JS, Jung HS (2007) Fomitopsis incarnatus sp. nov. based on generic evaluation of Fomitopsis and Rhodofomes. null 99:833–841. https://doi.org/10.1080/15572536.2007.11832515

Kornerup A, Wanscher J (1981) Methuen handbook of color

Li H, Cui B-K, Dai YC (2014a) Taxonomy and multi-gene phylogeny of Datronia(Polyporales, Basidiomycota). Persoonia 32:170–82. https://doi.org/10.3767/003158514X681828

Li H-J, Han M-L, Cui B-K (2013) Two new Fomitopsis species from southern China based on morphological and molecular characters. Mycological Progress 12:709–718. https://doi.org/10.1007/s11557-012-0882-2

Li H-J, Li X-C, Vlasák J, Dai Y-C (2014b) Neofomitella polyzonata gen. et sp nov., and N. fumosipora and N. rhodophaea transferred from Fomitella. Mycotaxon 129:. https://doi.org/10.5248/129.7

Lutzoni F, Kauff F, Cox CJ, et al (2004) Assembling the fungal tree of life: progress, classification, and evolution of subcellular traits. American Journal of Botany 91:1446–1480. https://doi.org/10.3732/ajb.91.10.1446

Maddison D, Maddison W (2005) MacClade 4: Analysis of phylogeny and character evolution. Version 4.08a.

Mason-Gamer RJ, Kellogg EA (1996) Testing for Phylogenetic Conflict Among Molecular Data Sets in the Tribe Triticeae (Gramineae). Systematic Biology 45:524–545. https://doi.org/10.2307/2413529

Masuka A, Ryvarden L (1993) Two new polypores from Malawi. Mycologia Helvetica 5:143–148

Mossebo DC, Ryvarden L (1997) Fomitopsis africana nov. sp.(Polyporaceae, Basidio-mycotina). SYDOWIA-HORN- 49:147–149

Ortiz-Santana B, Lindner D, Miettinen O, et al (2013) A phylogenetic overview of the Antrodia clade (Basidiomycota, Polyporales). Mycologia 105:. https://doi.org/10.3852/13-051

Pegler DN (1996) Hyphal analysis of basidiomata. Mycological Research 100:129–142. https://doi.org/10.1016/S0953-7562(96)80111-0

Posada D, Crandall KA (1998) MODELTEST: testing the model of DNA substitution. Bioinformatics 14:817–818. https://doi.org/10.1093/bioinformatics/14.9.817

Rambaut A, Drummond A (2007) Tracer 1.4

Reeb V, Lutzoni F, Roux C (2004) Contribution of RPB2 to multilocus phylogenetic studies of the euascomycetes (Pezizomycotina, Fungi) with special emphasis on the lichen-forming Acarosporaceae and evolution of polyspory. Molecular Phylogenetics and Evolution 32:1036–1060. https://doi.org/10.1016/j.ympev.2004.04.012

Rivoire B (2020) Polypores de France et d'Europe, MYCOPOLYDEV, Orleans, France

Ronquist F, Teslenko M, van der Mark P, et al (2011) MrBayes 3.2: efficient Bayesian phylogenetic inference and model choice across a large model space. Systematic Biology 61:539

Rungjindamai N, Pinruan U, Hattori T, Choeyklin R (2008) Molecular characterization of basidiomycetous endophytes isolated from leaves, rachis and petioles of the oil palm, Elaeis guineensis, in Thailand. Fungal Diversity 33:139–161

Ryvarden L (1972) A critical checklist of the Polyporaceae in tropical East Africa. Norw J Bot 19:229–238

Ryvarden L, Aime MC, Baroni TJ (2009) Studies in neotropical polypores 26. A new species of Trametes and revisitation of an old. Synopsis Fungorum 26:27–32

Ryvarden L, Gilbertson R (1994) European Polypores 2. Meripilus-Tyromyces. Synopsis Fungorum 7., Oslo, Norway: FungiFlora

Ryvarden L, Johansen I (1980) A preliminary polypores flora of east Africa, Oslo, Norway: FungiFlora.

Ryvarden L, Melo I (2014) Poroid fungi of Europe. Fungiflora

Simmons MP, Pickett KM, Miya M (2004) How meaningful are Bayesian support values? Molecular Biology and Evolution 21:188–199. https://doi.org/10.1093/molbev/msh014

Spirin V, Vlasák J, Miettinen O (2017) Studies in the Antrodia serialis group (Polyporales, Basidiomycota). null 109:217–230. https://doi.org/10.1080/00275514.2017.1300087

Spirin V, Vlasák J, Rivoire B, et al (2016) Hidden diversity in the Antrodia malicola group (Polyporales, Basidiomycota). Mycological Progress 15:. https://doi.org/10.1007/s11557-016-1193-9

Stamatakis A, Hoover P, Rougemont J (2008) A Rapid Bootstrap Algorithm for the RAxML Web Servers. Systematic Biology 57:758–771. https://doi.org/10.1080/10635150802429642

Thiers B (2016) Index Herbariorum: A global directory of public herbaria and associated staff. New York Botanical Garden's Virtual Herbarium. http://sweetgum nybg org/ih

Vlasák J, Vlasák JrJ, Ryvarden L (2016) Studies in neotropical polypores 42. New and noteworthy polypores from Costa Rica and two new species Elmerina phellinoides and Melanoporia condensa. Synopsis Fungorum 42:9–33

Vu D, Groenewald M, de Vries M, et al (2019) Large-scale generation and analysis of filamentous fungal DNA barcodes boosts coverage for kingdom fungi and reveals thresholds for fungal species and higher taxon delimitation. Studies in Mycology 92:135–154. https://doi.org/10.1016/j.simyco.2018.05.001

Wang Z, Binder M, Dai Y-C, Hibbett D (2004) Phylogenetic Relationships of Sparassis Inferred from Nuclear and Mitochondrial Ribosomal DNA and RNA Polymerase Sequences. Mycologia 96:1015–29. https://doi.org/10.2307/3762086

White F (1986) La végétation de l'Afrique : mémoire accompagnant la carte de végétation de l'Afrique UNESCO/AETFAT/UNSO. ORSTOM ; UNESCO, Paris

Xia X, Lemey P (2009) Assessing substitution saturation with DAMBE. In: Vandamme A-M, Salemi M, Lemey P (eds) The Phylogenetic Handbook: A Practical Approach to Phylogenetic Analysis and Hypothesis Testing, 2nd edn. Cambridge University Press, Cambridge, pp 615–630

Xia X, Xie Z (2001) DAMBE: Software Package for Data Analysis in Molecular Biology and Evolution. Journal of Heredity 92:371–373. https://doi.org/10.1093/jhered/92.4.371

Xia X, Xie Z, Salemi M, et al (2003) An index of substitution saturation and its application. Molecular Phylogenetics and Evolution 26:1–7. https://doi.org/10.1016/S1055-7903(02)00326-3

Yombiyeni P, Douanla-Meli C, Amalfi M, Decock C (2011) Poroid Hymenochaetaceae from Guineo–Congolian rainforest: Phellinus gabonensis sp. nov. from Gabon – taxonomy and phylogenetic relationships. Mycological Progress 10:351–362. https://doi.org/10.1007/s11557-010-0708-z

Figures

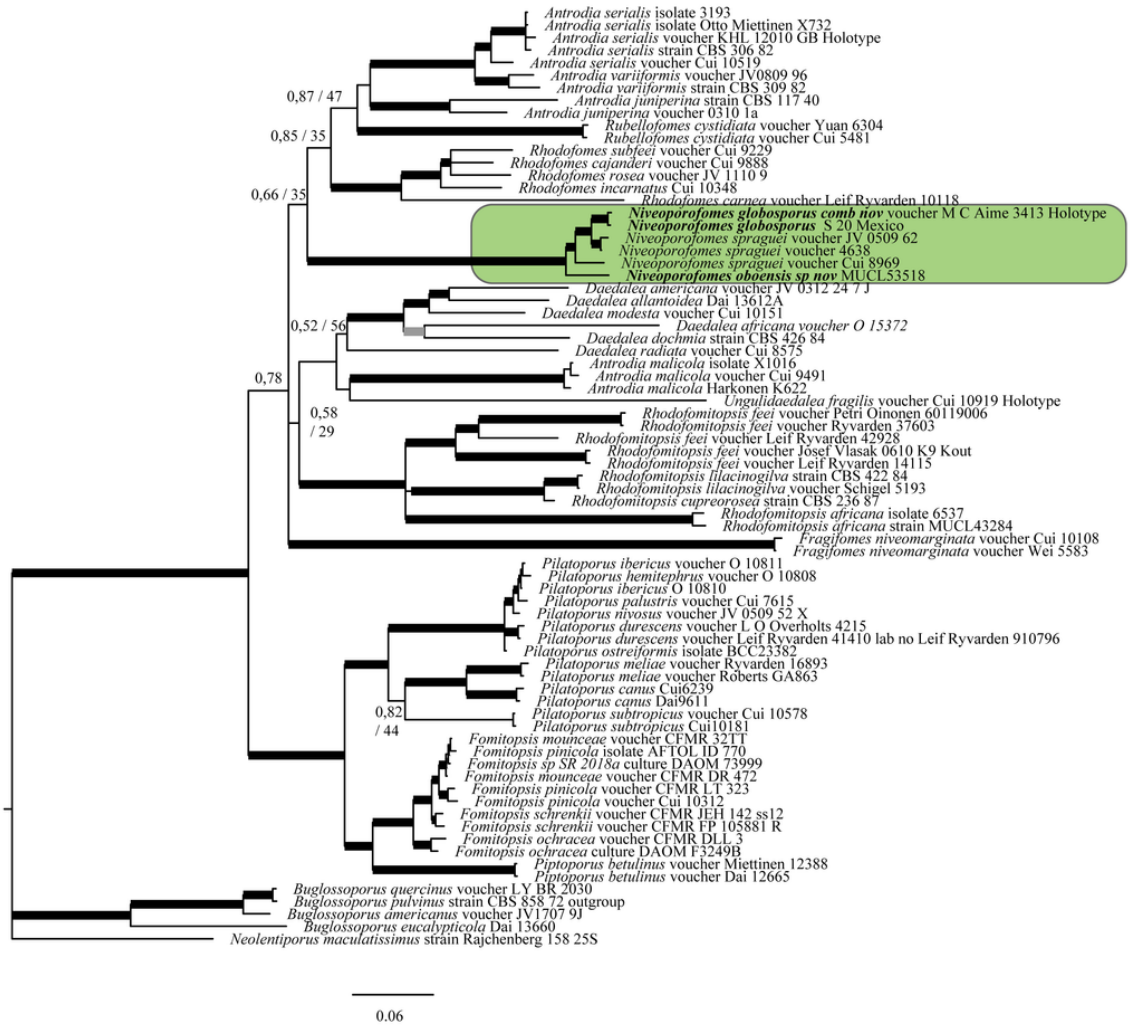

Figure 1

The 50% majority-rule consensus tree from Bayesian inference of the combined dataset. Thickened branches in bold represent ML BS support greater than 75% and BPP greater than 0.95; thickened branches in grey denote branches supported by either ML BS or BPP; For selected nodes ML BS support value and BPP are respectively indicated to the left and right of slashes; The new taxa are highlighted in the shaded box.

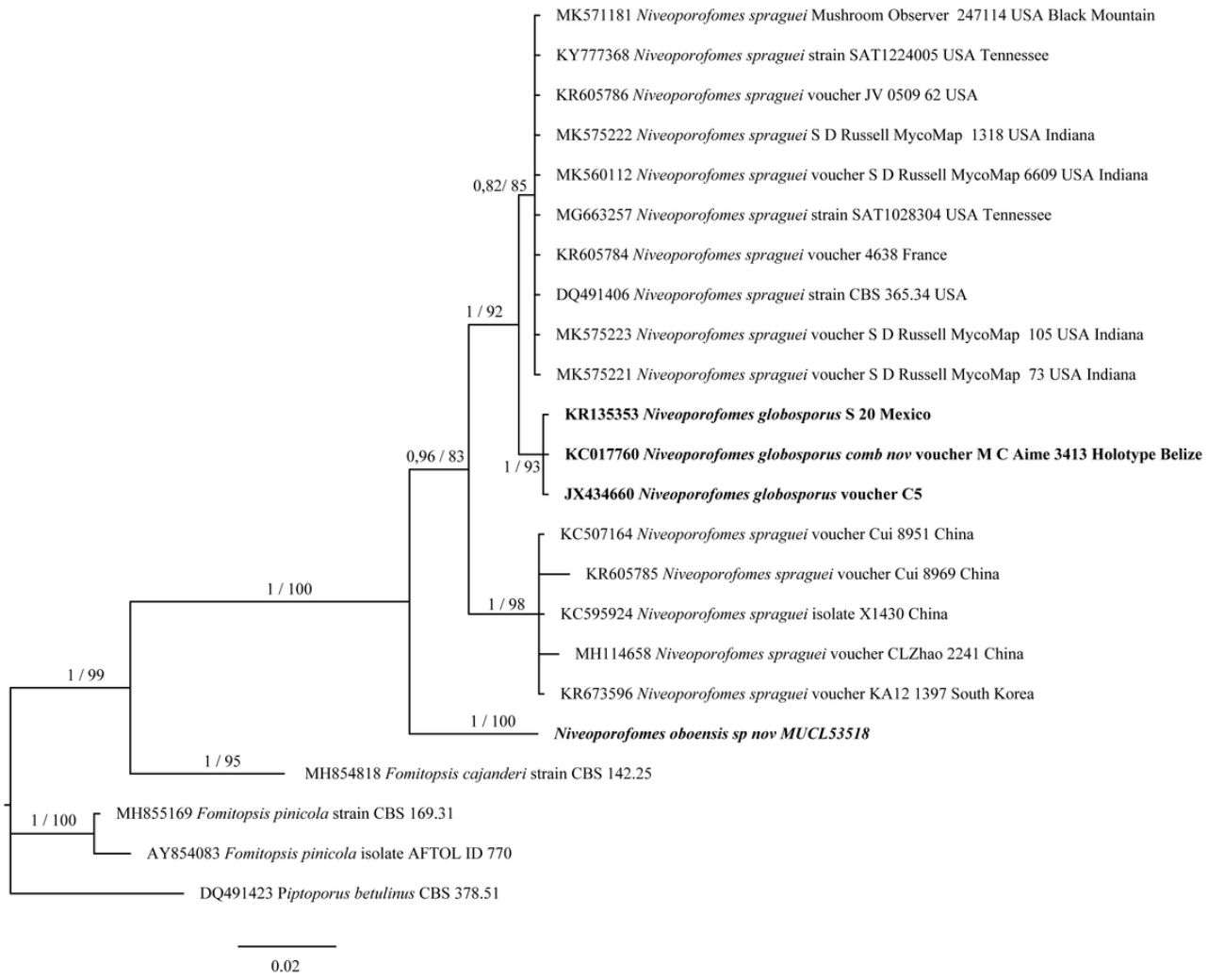

Figure 2

Bayesian Inference consensus tree based on ITS sequence data for species of Niveoporofomes, with Piptoporus betulinus strain CBS 378.51 as outgroup. Posterior probabilities obtained through Bayesian inference and bootstrap values (1000 replicates) obtained from Maximum Likelihood analysis are respectively indicated to the left and right of slashes.

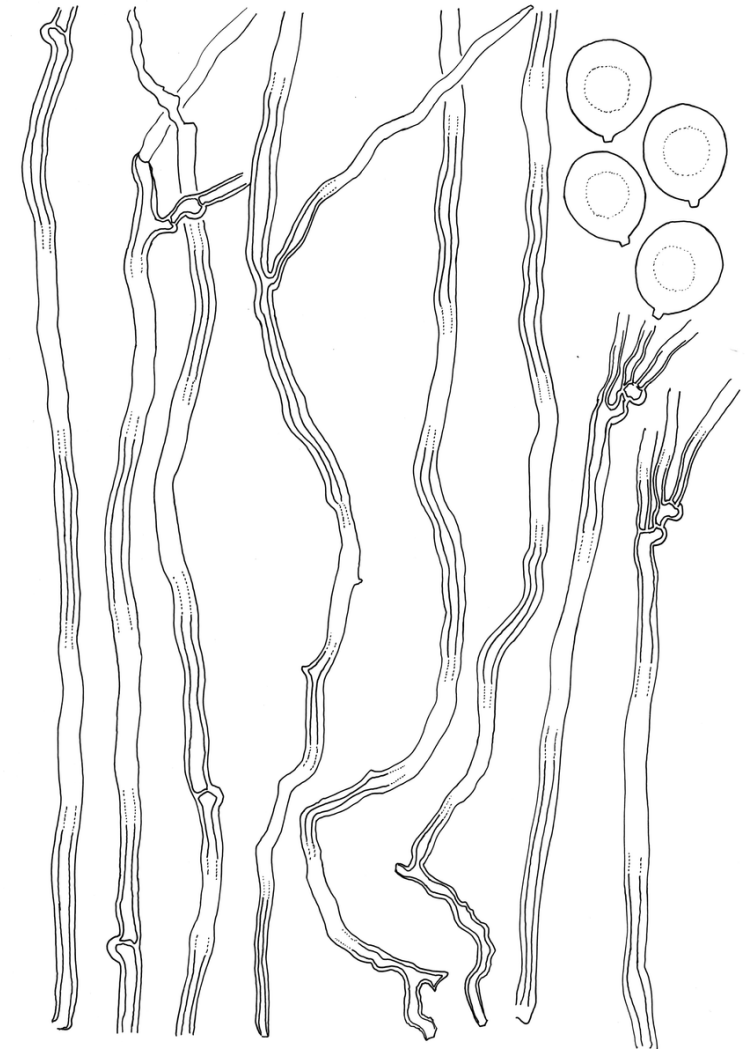

Figure 3

Niveoporofomes oboensis, from type ST/11-04, MUCL 56368. Vegetative hyphae from the hymenophoral trama (scale bar = 25 µm).

Supplementary Files

This is a list of supplementary files associated with this preprint. Click to download.

- OnlineResource1.nex
- OnlineResource2.nex